Upper Limb Exoskeleton for Shoulder Joint Control

Colton Applegate
Department of Mechanical and Aerospace Engineering
University of Virginia
Charlottesville, VA
cta2zn@virginia.edu

Joseph Carley
Department of Mechanical and Aerospace Engineering
University of Virginia
Charlottesville, VA
j4eb@virginia.edu

Nazirah Farach Rojo
Department of Mechanical and Aerospace Engineering
University of Virginia
Charlottesville, VA
nf5ay@virginia.ed

Marvin Lee
Department of Mechanical and Aerospace Engineering
University of Virginia
Charlottesville, VA
ml3zv@virginia.edu

Isabella Nazari
Department of Mechanical and Aerospace Engineering
University of Virginia
Charlottesville, VA
iln9nt@virginia.edu

Abstract*—There is a need for soft, flexible upper-limb exoskeletons for patients with muscular dystrophy. Using pneumatic actuators will create a more comfortable design that achieves multiple degrees of freedom in the shoulder joint. This paper discusses the current literature on exoskeletons, the process used to design the current model consisting of a support brace and various artificial muscles, and the testing performed on the system. Two different artificial muscle types are tested to compare the performance and durability when actuated. The use of soft artificial muscles will hopefully improve the user experience and provide assistance with everyday tasks.

***Keywords*—exoskeleton, pneumatic actuators, flexible, upper limb, soft robotics, wearable electronics, mesh, artificial muscle**

I. Introduction

According to the National Organization for Rare Disorders, there are around 250,000 individuals in the United States alone that suffer from some degree of muscular dystrophy (MD) [1]. Upper limb motility in particular is crucial to a patient's independence, self-esteem, and quality of life. While the loss of lower extremity function can be largely compensated for with a wheelchair or prosthetic device, there are very few options available for patients with reduced muscle ability in their upper body [2]. More recently, mechatronic exoskeletons are being developed to provide powered motion to patients. This approach has many advantages including the potential for completely motor driven, patient controlled movement. Current systems widely use a 5 degree-of-freedom (DOF) motor driven rigid system, which while able to achieve accurate motion, suffers from several drawbacks including bulkiness, weight, and power consumption.

There are many mechanical exoskeleton prototypes on the market, but most of them are missing key elements to make them sufficiently helpful to people with MD. For example, most exoskeletons cannot achieve a rotational DOF, nor are they comfortable for the patient to wear. The goal of this project is to design an upper-limb exoskeleton to assist patients with neuromuscular disorders in performing everyday motions. There are three teams involved in this project, and this specific one is focusing on the shoulder joint and how to replicate the motion of a human shoulder using soft materials. The shoulder has three degrees of freedom. The first one, flexion and extension, relates to the sagittal plane and moves the arm back and forth. The second is abduction and adduction, which deals with the frontal plane and moves the arm from side to side. The last, and most complicated degree of freedom, is the medial-lateral rotation of the shoulder. The main motivation for this design is to achieve the abduction and adduction range of motion in the shoulder while still using soft materials rather than hard motors.

The majority of current exoskeletons designs use DC motors and a rigid external structure to achieve the 3 DOF located in the shoulder. While there are many current designs using hard actuators, there is a noticeable lack of research on the use of flexible actuators and sensing systems to create wearable technologies that move more naturally with a human arm. By creating a soft exoskeleton, patients can have more comfort when performing everyday tasks. The question that this research aims to solve is: How can a flexible, soft upper-limb exoskeleton be created to enable patients to move independently in order to perform daily tasks?

II. Review of Literature

While the applicable range of exoskeletons covers a variety of different uses, the largest category are upper-limb devices designed specifically for physical therapy. The main problem with most exoskeletons in this category is that they are made with rigid joints and kinematic constraints which can create hyperstaticity, or an excessive amount of support components. While this is a problem that can be overcome, if handled incorrectly it can result in prototypes that are unsafe and unsuitable for patient use [3]. Due to the potential problems this type of exoskeleton can cause, there has been an increased demand to transition from hard actuators to soft actuators, as soft actuators are less likely to cause injury to a patient if a malfunction occurs.

A. *Passive Assistive Systems*

Passive assistive systems utilize different mechanisms including springs and tendons to reduce the amount of force required by the patient to perform a particular motion. One such system developed by Honda reduces the effort required to walk through the use of a

passive spring element and specifically designed clutches [4]. Myosuit is another system developed using tendon actuators and shown to reduce the energy cost of walking by 6.4% [5]. These passive designs benefit from the absence of complex sensing and actuating systems which cause lag between the control and output of the patient's movement. While limited in the mechanical support they can provide, the simplicity and repeatability of these designs has proved useful in assisting patients with lower body MD, and could potentially be applied to patients with upper limb MD.

B. Artificial Muscles

a. Soft Actuators

One of the newest advancements in creating a softer exoskeleton system is the implementation of pneumatic artificial muscles. Artificial muscles mimic the expansion and contraction of human muscles by inflating and deflating. Prior studies have achieved moderate success in prototypes utilizing them, but the range of motion has been limited, and fluid movement has been restricted by the greater difficulty in controlling artificial muscles when compared to DC motors [6]. Despite these hurdles, advancements have been made in decreasing the size of pneumatic artificial muscles and finding new ways to increase the range and types of motion.

Aside from pneumatic actuators, there are several other types of soft actuators that can achieve similar functions. One example of this is the elastomeric fluid actuator, which acts similarly to muscles when actuated, and resembles the flexibility of the upper-body when unactuated [7]. An advantage of this type of actuator is that it allows for large-scale deformation, and relatively high compliance compared to traditional rigid-bodied exoskeletons. However since these actuators expand and contract by filling with a fluid, they typically end up requiring the system to be much heavier and therefore uncomfortable for the patient.

In a study by Das and Kurita, pneumatic gel muscles were used rather than traditional pneumatic actuators. One major drawback of using traditional pneumatic actuation for artificial muscle design is the need for heavyweight compressors [8]. While the gel model was more lightweight that some other ones, only one DOF, shoulder flexion,was achieved, and therefore the model was not able to assist in performing various everyday tasks.

b. Cables

Another popular design for artificial muscles includes the use of cables rather than actuators. The cables are controlled by DC motors. Lessard et al. chose the placement of the cables by developing paths along the most important muscle groups and achieved flexion/extension and abduction/adduction of the shoulder joint [9]. In a review of upper-limb exoskeletons, a five DOF design was discussed that also used hard motors in a cable-driven system. All three DOFs in the shoulder were achieved, but the model was not flexible and did not use pneumatic actuation [10].

III. MOTIVATION

The primary objective of this research project is to develop a soft, upper limb wearable exoskeleton that incorporates soft pneumatic actuators to enable patients to live more independently and perform daily tasks. This subteam will focus on the design, fabrication, and testing of the robotic shoulder joint. In order to guide this research, two major underlying questions will be carefully discussed during the design process. First, how can the abduction and adduction DOF be achieved by using soft materials, and second, what designs of artificial muscles can be used to provide the forces that are required to control the shoulder joint? The physical placement of the artificial muscles will also be studied in order to provide the desired DOF and various motions that are trying to be imitated.

IV. ARTIFICIAL MUSCLE BACKGROUND

A. McKibben Muscles

The regular McKibben Muscle is produced by weaving a fabric into a mesh pattern, and wrapping this fabric outside of an internal inflatable bladder, which can then expand and contract with the mesh. The driving factors of this design are the angle in which the mesh is weaved together, and the internal diameter of the bladder.

B. Fishing Line Muscle

The Fishing Line Muscle was based on previous research that claimed a max achievable elongation of 300% [11]. What makes this muscle so much different from McKibben based muscles is the way it expands and contracts. Traditional McKibben Muscles are at their longest in their deflated state, and when inflated they contract. The fishing line muscle does this opposite, where it elongates with inflation rather than deflation.

C. Designing the Mesh for McKibben Muscles

Figure 1 displays the characteristics of the outer braided mesh utilized in the muscle. According to Tondu et al., there are m columns and n rows whose envelope is a rectangle of initial length l_0 and width L_0. The initial angle of each elementary pantograph is denoted as α_0. As the angle increases and the rectangular shape is maintained, the width L increases while the length l decreases. Assuming that the side of each 'bent' pantograph, noted s, can effectively remain constant during the 'contraction/elongation' process, the length l and radius r can be determined shown in Eq. (1) as a function of the mesh angle:

$$\frac{r}{r_0} = \frac{\sin\alpha}{\sin\alpha_0} \; and \; \frac{l}{l_0} = \frac{\cos\alpha}{\cos\alpha_0} \qquad (1)$$

Using Eq. (1), the contraction function, Eq. (2), is found:

$$f(\varepsilon) = \frac{1}{\sin \alpha_0}\sqrt{1 - \cos^2\alpha_0(1 - \varepsilon)^2} \qquad (2)$$

$$\frac{r}{r_0} = f(\varepsilon) \; where \; \varepsilon = \frac{(l_0 - l)}{l_0} \qquad (3)$$

If the general muscle force equation is applied to this contraction function, Eq. (4) , the output force of an ideal pneumatic artificial muscle, is produced as a function of the strain, ε, and internal pressure, P:

$$F(\varepsilon) = (\pi r_0^2)P[a(1 - \varepsilon)^2 - b] \qquad (4)$$

$$where \; a = \frac{3}{\tan^2\alpha_0} \; and \; b = \frac{1}{\sin^2\alpha_0} \quad .$$

It was found that the artificial muscle will increase in length when the mesh angle is greater than 54.44 degrees, and it will decrease in length when it is below this threshold angle. In order to mimic a natural muscle, it is critical that an angle less than 54 degrees is chosen to create contraction, rather than expansion [12].

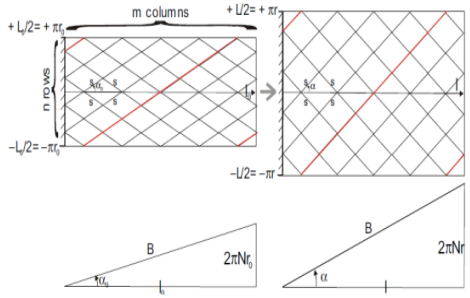

Fig. 1. Geometrical characterization of the braided sheath of the McKibben muscle [12].

There are many different meshes on the market, with different mesh angles, diameters, and materials. For the prototype, a mesh angle needs to be determined. Using Matlab and the equation in Figure 2, the best angle was determined. This was achieved by setting values to the initial diameter (D_0), initial length (L_0), change in length (ΔL), and pressure (P). Force (F) was set as the dependent variable, and the angle (θ) was set as the independent variable. From an initial prototype design, the measurements of the adduction/abduction artificial muscle A, as seen in Figure 2, were recorded. L_0 was found to be 18.415 cm, and ΔL was measured to be 5.715 cm. The diameter was set to be 3 cm. The internal pressure was set to 500 N/cm^2, as this is commonly used in the design of thin McKibben Muscles [13].

The mesh angle has been determined to be around 22.753 degrees by looking at Figure 3, and the width of the inner tube will be in the range of 0.5 to 0.75 inches. The current plan is to either buy a mesh to fit these parameters, or fabricate it in-house if no suitable material is found. A potential design with a mesh angle of 22.753 degrees is shown in Figure 4.

$$F = \left(\frac{\pi D_0^2 P}{4}\sin^2\theta_0\right)\left[3\left(1 - \frac{\Delta L}{L_0}\right)^2\cos^2\theta_0 - 1\right]$$

where F is the generated force, P is the given air pressure, $\Delta LL/LL$ is the contraction, and the others are geometry parameters

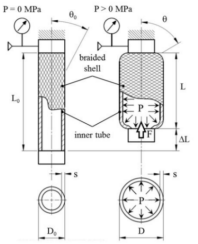

Fig. 2. Calculation of force the artificial muscle can exert depending on initial angle, pressure, initial length, and change in length.

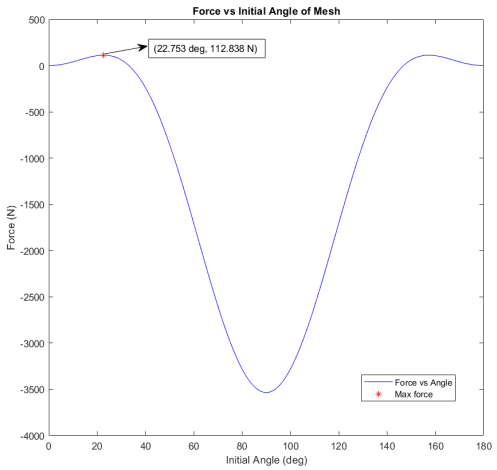

Fig. 3. Force vs. Initial Angle of Mesh. This graph shows the relationship between the generated force and the angle of the mesh, showing that the highest force generated with an angle of 22.753 degrees.

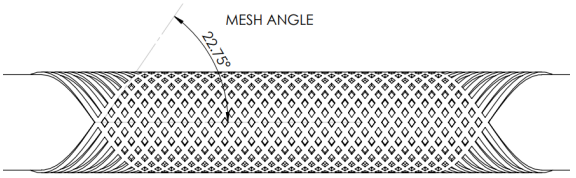

Fig. 4. Potential Design of Fabricated Mesh

To re-evaluate the angle obtained from the graph in Figure 3, the equation shown in Figure 2 was used to create the graph in Figure 5. This graph shows the relationship between the initial diameter, D_0, and the angle of the mesh. The equation in Figure 4 was re-arranged as follows:

$$D_0 = \left[\frac{F}{(\pi P \sin^2(\theta_0))(3(1 - \frac{\Delta L}{L_0})^2\cos^2(\theta_0) - 1)}\right]^{1/2} \qquad (5)$$

Eq. (5) was graphed using similar parameters as used for Figure 5, however this time F was set to 10 N, which can be seen in Figure 5. As shown on this graph, the smallest diameter is also obtained with an angle of 22.753 degrees. By doing several iterations, it was shown that the smallest diameter will always be at 22.753 degrees with the set values, but depending on the needed force the diameter will change, increasing as the force increases.

To determine the force of the whole shoulder, the principle of superposition can be applied to the force output

of each individual muscle. EMG sensors will be placed on each muscle to estimate the force needed to provide the necessary motion. The muscles that are currently being looked at are the trapezius, deltoid, pectoralis major, triceps, and biceps. Once a force range is established, an additional 20 Newtons will be added to the force, to ensure that the exoskeleton can not only lift the arms, but also day-to-day objects.

With a finalized force range for each of the muscles, Figure 6 was created to find the pressure needed to exert the desired force.

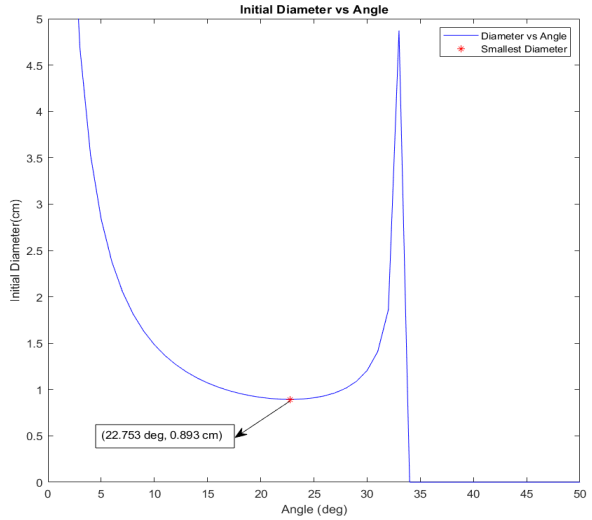

Fig. 5. Initial Diameter vs. Angle. This graph shows the relationship between the initial diameter and the angle of the mesh, showing the ideal angle shown in Figure 3.

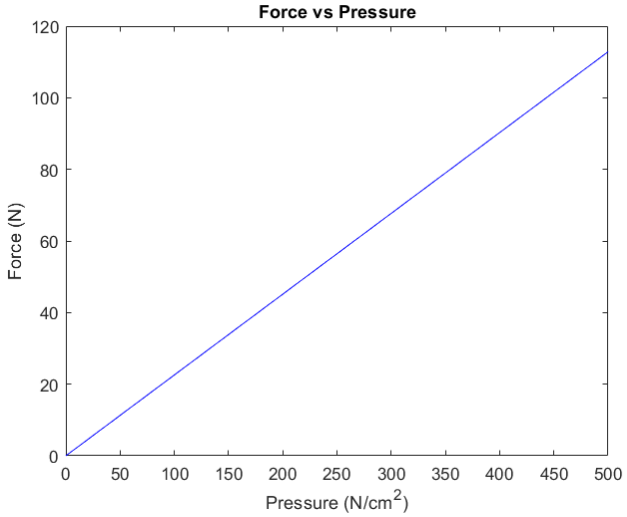

Fig. 6. Force vs. Pressure of Bladder. This graph shows the relationship between the internal pressure of the bladder with the output force, using an angle of 22.753 degrees, and the same parameters used for the graph shown in Figure 4.

V. Methods and Materials

Based on the research conducted in the review of existing upper arm exoskeletons, it was determined that there were several possible options to pursue in the design for the exoskeleton. Within the realm of soft actuators alone, there are a plethora of different materials and designs that can be implemented into a soft actuator system. Therefore the first step in the design process was to decide on the type of individual artificial muscle to be used. There are two main designs of interest that were considered for this prototype, regular McKibben Muscles and Fishing Line Muscles.

A. Structural and Mechanical Design

a. Artificial Muscle Design

The first step in the prototyping phase was to create working artificial muscles that satisfied the design criteria. The first iterations of muscle designs produced were all McKibben style artificial muscles, meaning that each muscle consisted of an internal bladder and an external mesh. Several different bladder and mesh sizes were tested in this process, with the goal of maximizing the contraction ratio of the muscle. One of the first issues that was encountered was the inability of the air pump being used to produce a high enough internal air supply to effectively contract the muscles. The pump being used could only reach a maximum pressure of 12 psi, and the calculations that were done indicated that a pressure of at least 35 psi would be needed to achieve sufficient muscle contraction. The pump was eventually replaced with one capable of producing pressures up to 70 psi, but this quickly revealed a new problem in the design: air leakage. Up until this point, the muscles that had been designed used rubber bands, hot glue, and zip ties to seal the ends, all of which were not capable of producing a completely air tight seal. This caused a significant amount of air to leak out from the muscles, preventing them from achieving maximum contraction. This was improved upon by using heat-shrinking end caps, that effectively sealed the ends of the muscle, and allowed them to retain the air that was pumped into them. The design at this point was capable of achieving 10-20% contraction, which was much less than originally desirable, but an acceptable place to start. This design is shown in the bottom of Figure 7, where the previous design interactions can be seen above it. Note that in this design a ball pump needle was being used to connect the muscle to the air supply, which also helped create an airtight connection with the pump.

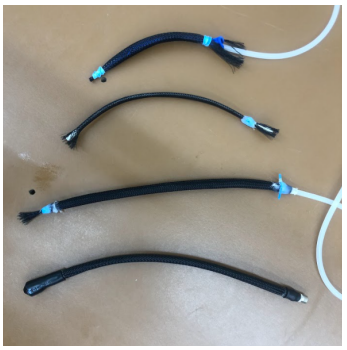

Fig. 7. Iteration of artificial muscle designs in chronological order from top to bottom.

b. Shoulder Brace

The next step in the design process was to figure out how to mount these muscles onto the human user. For the initial design of these mounting points, a variety of commercially available vests and harnesses were purchased. The harnesses were tested for ease of use, how well the straps stayed in place when forces were applied, the availability of mounting points, and comfort. Through evaluating these parameters, it was quickly clear that currently available devices would not suffice. This meant that a custom harness system would need to be developed, using a mix of purchased and custom designed 3D printed parts. A medical sling device was purchased to serve as the basis of the system, as it consisted of a shoulder brace and arm support, both necessary components to attach the artificial muscles to. The problem with this device is that there was no way to attach the artificial muscles to it, so a 3D printed muscle mount was designed to adapt the muscles to the nylon strap system of the medical sling. Several of these mounts, shown in Figure 8 were printed, as each muscle required 2 to be properly held in place.

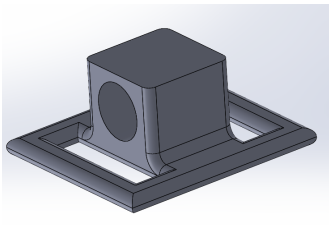

Fig. 8. 3D Printed Mount

For the first prototype, it was decided that 3 artificial muscles should be used, as it was estimated that one muscle by itself would not be able to generate sufficient force to actuate the shoulder. At this stage of design a new problem was introduced. Up until now each artificial muscle had been tested and used individually via a screw-on connection to the electric air pump. Testing this design required all three muscles to be powered simultaneously, with one air supply. To achieve this, an alternate connection point was installed on the muscles, and plastic tubing was used in conjunction with T connectors to deliver equal air pressure to all three of the muscles at once via one pump. Once the muscles were connected and secured to the medical sling, the first actuation tests were conducted on a human subject. See Fig 9. for the fully constructed prototype.

Fig. 9. Initial Prototype. This figure shows the prototype in place on a test subject, with tubing and pump connected.

Using this design, a small degree of adduction was achieved, though the motion more closely resembled a shoulder shrug. There was noticeable slippage in the bicep mounting strap, and from the shoulder, likely attributing to the reduced movement of the actual arm of the subject. To reduce this slippage, a design that better fixed to the patient's upper arm was required.

In this initial round of testing, it was noted that as the muscles contracted, they would pull the shoulder brace and arm bands closer together as expected, but both supports would just slide either up or down the arm. In order to actually move the subject's arm with the contraction of the muscle, it was imperative that the support braces stay in place relative to the arm, so the contraction motion generated by the muscles provides motion to the arm, and not to slippage of the braces. To accomplish this, it was necessary to redesign the support system from scratch, again using 3D printed parts since there was nothing on the market sufficient for the design. The goal for this next iteration of design was to produce a solid plastic shoulder support brace, which could then be held in place by support straps attached to the user's waist. Although the initial goal of this project was to use as few rigid components as possible, it was deemed necessary to use a plastic support brace for the shoulder, as the muscles needed a rigid attachment point in order to stay in place. However, the design was carefully modeled to match the human shoulder contour as closely as possible to maximize comfort. As shown in Figure 10, this design was printed in two separate halves, which could then be connected together via screws once in place around the user's neck. Several holes were also left for each half of the brace, to allow for a modular system of muscle point attachments, as attachments could be attached and removed with ease, without having to reprint the base muscle structure.

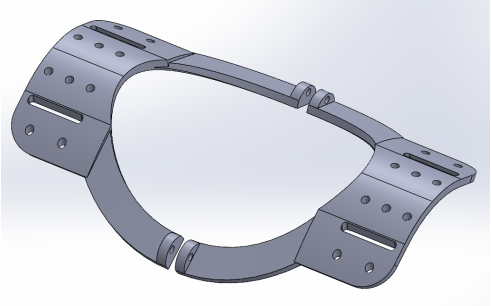

Fig. 10. 3D Printed Shoulder Brace Prototype

Two slots were also left on each side of the model, where the nylon straps would then be fed through and down to the user's waist. These nylon straps were then fastened to the user's belt, and could then be adjusted and tightened based on the size and height of each user. The straps were fed vertically down from the brace to the belt, and the tension created by this arrangement generated enough of a frictional force to prevent sideways movement of the brace during muscle actuation. While not a perfectly designed model, the test subject reported moderate comfort over an extended period of wear.

The next phase of development was to design and print the muscle attachment points to secure the muscles to the shoulder brace. It was quickly realized during the development of the attachment point, that the muscle has to be elevated slightly from the surface of the brace. As demonstrated by the first prototype, when the muscle sat perfectly along the user's shoulder and arm, the resultant motion was more of a shrug motion than an adduction motion. This is because the actuation force was acting in the same direction as the arm, meaning that only a vertical force could be generated. To achieve abductive and adductive motion, a portion of the actuation force needs to act perpendicularly to the arm, in order to pull the arm away from the user's body. By offsetting the muscle attachment point a few inches off of the user's arm, enough perpendicular force was generated to successfully actuate the arm in the adductive motion. For simplicity in this stage of development, it was decided that only one artificial muscle would be used.

Another issue that had to be addressed was replication of the curvature of the shoulder in the attachment point design, as the artificial muscle needed to be smoothly guided along the user's arm to allow for seamless actuation. There was also trouble keeping each mount in place using just the hole and peg layout that was originally developed, so an attachment clip was developed on later iterations to help secure the mount to the brace. Lastly, 3D printed clips were designed to keep the actual artificial muscles in place, using screw attachment points. Figure 11 shows the design iteration process of the shoulder mount piece before landing on the final design.

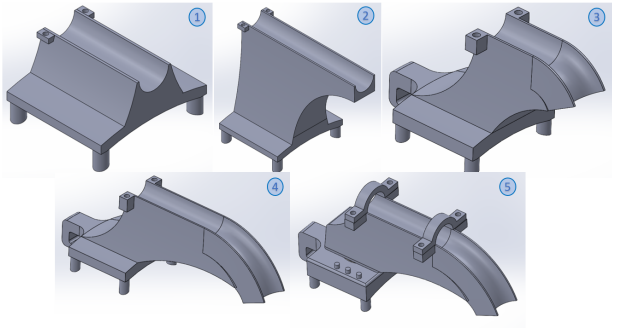

Fig. 11. Shoulder Mounting Design Iterations

One final flaw in the design that was realized late in development was that the designs produced thus far had been fixed to only actuate the shoulder in the adduction/abduction direction, and the user could not rotate their arm freely. This was resolved in the final iteration of the muscle mount, where a bearing was used to allow free rotation of the user's arm, whether the artificial muscle was actuated or not. The final design is shown in Figure 12.

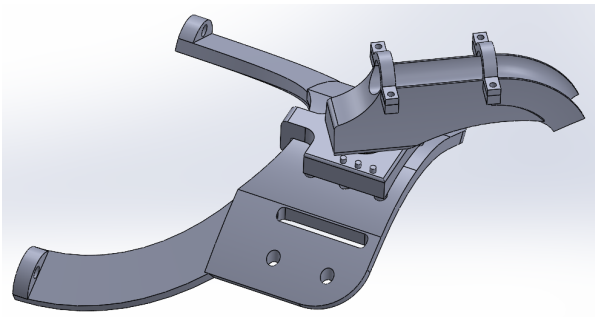

Fig. 12. Final Iteration of Shoulder Mount

With the design for the shoulder brace complete, the next step in development was to develop a method to attach the artificial muscle to the arm support brace, another significant cause of slippage as discovered from the initial testing. Several options were tested to create a model that stayed in place relative to the user's arm, including tight arm bands and 3D printed plastic pieces. Unfortunately, all of these designs fell victim to the same problem, where no matter how tight or rigid the models were to the skin, they would still slide up the user's arm. This is because skin is inherently elastic, and any design produced would be prone to moving with the skin unless an external force was applied to keep it in place. This was resolved through the use of a purchased elbow brace that strapped around a user's arm both above and below the elbow. This meant that if a force

was applied above the elbow, the brace would not slip with the skin since a counter force was being provided by the straps below the elbow. While the use of this design added significantly more bulk to the system than originally desired, it was the only feasible way to ensure the arm attachment point would not slip during muscle actuation.

Although since this was a commercially purchased product, the elbow brace did not have any compatible attachment points for the artificial muscle. Additionally, the way the brace was designed was not conducive to any sort of 3D printable attachment points, which made securing the muscle to the brace even more difficult. Eventually, a system of zip tie attachments was used to secure the muscle in place, and although it was not the most elegant solution, it did provide consistent and reliable results. Figure 13 shows the complete muscle assembly with all components of the system, both in an actuated and unactuated state.

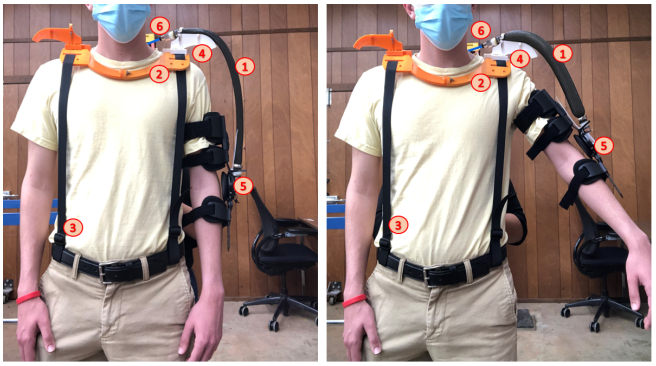

Fig. 13. System Assembly While Idle (left) and Actuated (right)
(1) McKibben Style Artificial Muscle (2) A 3D printed shoulder support brace that provides an attachment point for the artificial muscles (3) A strap system that keeps the shoulder brace from sliding out of place and can be adjusted based on the user (4) A 3D printed muscle mount that guides the artificial muscle's expansion direction (5) A purchased arm brace that provides an attachment point on the upper arm for the bottom end of the artificial muscle (6) Input Air supply to the artificial muscle

The completed design for the artificial muscle was originally designed to be a McKibben style of artificial muscle, but as previously stated this muscle was unable to generate the contraction ratio that was desired. At this point, the muscle design itself was reworked to see if a larger contraction ratio could be achieved. In the initial working prototype that used McKibben Muscles, a ¼" inner bladder was used with a ⅜" outer mesh. This muscle was able to achieve around 10-20% contraction reliably, which was much less than what was desirable. It was decided that this design could be improved upon by using a larger inner bladder of ½", and a larger outer mesh of ¾". While this new design was certainly an improvement, it only marginally increased the maximum contraction to about 27% using an ideal pressure of 60 psi. The results from this test can be seen in full in the next section. So while the McKibben Muscle did provide reliable and consistent results, it did not quite hit the goal for the maximum contraction ratio, so another type of model was considered as a potential replacement.

This new type of muscle, referred to as the Fishing Line Muscle, was tested next. Because this muscle works inversely to the Mckibben Muscle it was hard to adapt this muscle to our current system. But the hardest part was the actual construction of the muscle itself. To create a fishing line muscle, fishing line has to be tightly wrapped around an internal bladder, which requires time and intense care to produce correctly. The ends then have to be carefully sealed with tightening metal clamps, and then capped to create an airtight seal. See Figure 14 for the completed design of a Fishing Line muscle. It should also be noted that the system of metal clamps and end caps was also applied to the previous version of the McKibben Muscle, to ensure more accurate data when comparing the two types of muscles.

Fig. 14. Final Mckibben Muscle Design (top) and Fishing Line Model (bottom)

c. Air Supply

There were numerous issues early on with air leakage from this muscle, as there were several potential points of leakage in each muscle that had to be checked. Another major problem with this design was that it required careful monitoring of the incoming air flow, as if the muscle was inflated too quickly the muscle could burst. To address this issue, modifications were made to the pump to allow for a greater range of control over the air flow. Initially, a manual 3-Way 2-Position pneumatic solenoid valve (TAILONZ PNEUMATIC) was used to control the direction of airflow into the muscle. This provided an easy method to be able to quickly connect a muscle to a pump and verify the performance of new prototypes. However, the major drawback to this design was the lack of control of the speed of the airflow. The solenoid's manual on/off button not only made it difficult to predict the motion of the muscle, but also would pose safety hazards, as the rapid inflation and deflation caused sudden jolts to the user's shoulder/arm. Additionally, the lack of air control made it very difficult to consistently test the Fishing Line Muscle, as damages were very frequent. Sudden releases of air produced slippage of the fishing line, resulting in tangles and gaps forming between the coils. In order to combat these challenges, a preliminary design was made to control the air flow both in

and out of the muscle shown in Figure 15. With this design for the air pump, it was possible to complete some testing on the Fishing Line Muscle. While this design couldn't achieve the 300% elongation as claimed by the research group that first developed it, it was able to achieve over double the contraction ratio of the Mckibben Muscle, at a max elongation of 62.5%. See the next section for full experimental data.

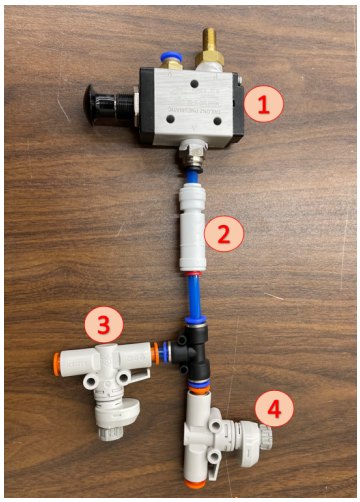

Fig. 15. Design to control air flow from the pump into the muscle. (1) Manual solenoid valve that can be opened and closed (2) One way check valve to prevent air from backtracking to the pump (3) Manual valve that controls the release speed of air from the muscle (4) Manual valve that controls the inflow of air to the muscle

VI. Evaluation Plan

To characterize the results of each of the muscle designs, two different tests were performed on each type of muscle. The first test was a simple expansion and contraction test to determine the change in length each muscle could achieve. This test was conducted by measuring the idle length of the muscle, and then filling it with different levels of internal pressure to measure the corresponding change in length. The goal of this test was to finalize the ideal internal pressure of the muscle, or the pressure value that yielded the most contraction before any additional pressure resulted in a negligible change in length. See Figure 16 for a sample McKibben Muscle test setup.

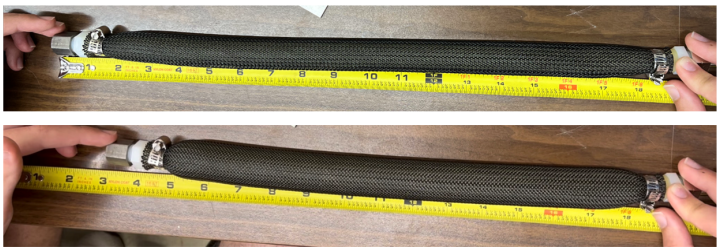

Fig. 16. McKibben Muscle Change in Length Test

The McKibben Muscle was tested first, and the results can be found in Table A. The ideal internal pressure was found to be 60 psi, which resulted in a maximum contraction ratio of 26.9%. The Fishing Line Muscle was then tested, which only required an ideal internal pressure of 30 psi, half of the McKibben Muscle. This muscle had an expansion ratio of 62.5%, which is more than double what the McKibben Muscle was able to achieve.

Table A: Results Summary of the Change in Length Test

Muscle Type	L0 (in)	ΔL (in)	Ideal Pressure (psi)	Contraction/Expansion Ratio
McKibben Muscle Inner-bladder Material:Latex ID: 1/2in OD: 5/8in Mesh Diameter: 3/4in	16.75	4.5	60	26.9%
Fishing Line Muscle Inner-bladder Material: Latex ID: 1/2in OD: 5/8in	7	4.375	30	62.5%

The other test that was conducted was an angle of actuation test, where each artificial muscle was attached to the support brace to measure it's actual effectiveness in practice. Since the primary goal of the project at this point was replicating the abduction/adduction degree of freedom in the shoulder, this was the DOF angle being measured in this test. To conduct this test, the muscle was affixed to the supporting brace structure using the designs layed out in the previous section. It had attachment points at both the shoulder mount as well as the elbow brace. The subject was asked to let their arm be completely at rest, and this point was set as the zero datum for measuring the angle of actuation. The muscle was then actuated and the final angle was recorded. The McKibben Muscle was tested first using the setup shown in Figure 17.

Fig. 17. Sample degree of freedom actuation test with the McKibben Muscle

This muscle was first inflated using a pressure of 10 psi, and then the angle of actuation was measured based on the end position of the user's arm. The test was then reset, and repeated in increments of 10 psi all the way up to the ideal pressure of 60 psi for the McKibben Muscle. A maximum angle of 45.5 degrees was achieved with 60 psi, and the results of each internal pressure are displayed in Figure 17. This angle seemed to be the absolute maximum achievable with the Mckibben Muscle, as any increase in pressure beyond 60 resulted in no further actuation.

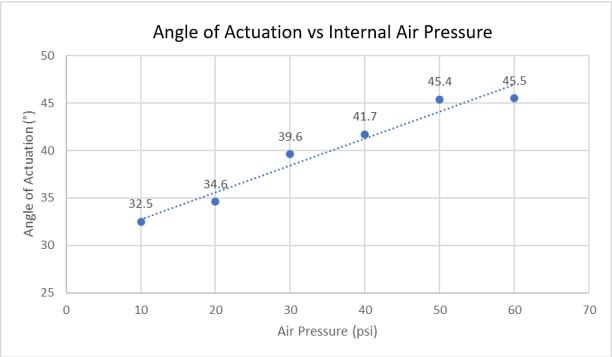

Fig. 17. Angle of actuation graph for the McKibben Muscle

The Fishing Line Muscle was also used in the angle of actuation testing, but due to the nature of how the muscle works the testing had to be modified. Because the muscle starts in its shortest state and expands from there, it had to be attached to the support system with the user's arm already raised. Once attached, the muscle was then inflated until the user's arm fell back into its natural resting position. Additionally, because the Fishing Line Muscle only works well with a very specific internal pressure, the only pressure level that was tested for this muscle was the ideal internal pressure of 30 psi. This resulted in only one angle being recorded for the fishing line muscle, which was 61.1 degrees of actuation. While this was significantly higher than the McKibben Muscle's max actuation, the Fishing Line Muscle was far less reliable, and its integrity was compromised after only a few test runs. It was therefore decided to stop testing the Fishing Line style of muscle, and use the more reliable McKibben Muscles for future work.

VII. Discussion and Conclusion

The primary objective of this project was to design and develop a wearable upper-limb exoskeleton using pneumatic actuators that assists users by controlling the shoulder joint. This project differs from previous research by solely using soft artificial muscles to control the shoulder joint rather than incorporating hard motors. The results of the experiments on both the artificial muscles and exoskeleton as a whole did not generate the level of actuation as expected, so it is recommended that future work should be conducted on muscle designs and placement.

In order to better understand the characteristics and performance of both the Mckibben and Fishing Line Muscles, further experimental testing is necessary. The relationship between pressure and force has been emphasized in many other studies, as this data is necessary to provide and predict the correct amount of assistance that the patient needs. A previous study that analyzed a similar muscle to the Fishing Line muscle utilized a device consisting of a force sensor, length sensor, and lead screws driven by a motor as shown in Figure 18 [14].

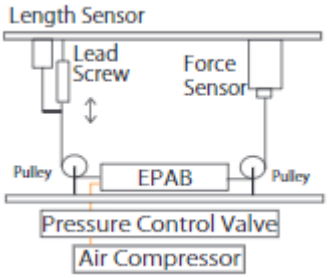

Fig.18. Potential setup to test force output [14]

Once a reliable experimental setup is established, other muscle parameters such as other inner bladder materials, mesh angles, and coil diameters/materials can be further studied. For example, a soft actuator reinforced with metal coil instead of a fishing line could be very applicable to the design presented in this study [15]. By testing other muscle designs, many benefits such as more force, range of motion, and overall muscle rigidity can be obtained.

Another aspect of this design that needs to be developed before it can achieve any practical use is the automatic inflation and deflation of the artificial muscles. In each of the tests performed during the development of this prototype, manual air pumps were used to inflate each muscle. This meant that an operator needed to be present to turn the air pump on and off when the muscles reached the desired state of inflation. To individually control the contraction of multiple muscles, a more elaborate air control system will be necessary. In this study, the pressure was measured solely by the pressure sensor inside the portable air pump. This pressure was likely not representative of the real-time state of the muscle, and during testing, major delays in the pressure readings were observed. A control system consisting of a PID controller, proportional valves, and pressure sensors is needed. Figure 19 displays a pressure control loop that has shown to be successful at controlling multiple artificial muscles used in a robot [16].

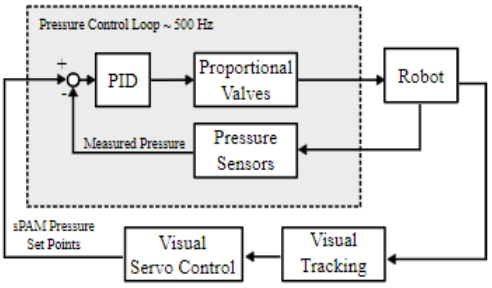

Fig. 19. Block diagram for pressure control system [16]

For this design to be effective when used with a patient, the artificial muscles need to be able to expand and contract automatically by reading the patient's muscle intention. There are a number of ways this can be achieved, but using Electromyography (EMG) sensors placed on key muscles located on the shoulder is recommended. By using EMG sensors, an algorithm that reads the muscle intention given off by a user's nervous system could then be written,

which would translate these signals into instructions for actuating the artificial muscles. Once complete, this would create an autonomous system that moves a user's arm completely based off of their motor intention.

Although the exoskeleton designed in this project partially achieves the adduction/abduction DOF in the shoulder joint, there is room for improvement in both this direction and the other two DOFs. Future research on this model would include creating stronger muscles that allow for a greater percent contraction, adding more muscles onto the system to account for additional weight, and achieving the other two DOFs in the shoulder joint. While this project was primarily focused on the shoulder joint, also adding the elbow and wrist joints would allow for a higher performing and more practical exoskeleton. This would involve incorporating muscles that actuate these joints and therefore can allow users to perform everyday activities that require multiple joints to be used simultaneously.

The use of exoskeletons for patients with MD can assist users with motor control and rehabilitation and also create a sense of independence. While much further research is required to get this technology to the point where it will be used in everyday life, the use of soft actuators in exoskeletons has the potential to dramatically improve the quality of life in MD patients.

References

[1] "Duchenne Muscular Dystrophy," *NORD (National Organization for Rare Disorders)*. https://rarediseases.org/rare-diseases/duchenne-muscular-dystrophy/ (accessed Dec. 17, 2021).

[2] S. D. Gasperina *et al.*, "Upper-limb actuated exoskeleton for muscular dystrophy patients: preliminary results," *Annu Int Conf IEEE Eng Med Biol Soc*, vol. 2019, pp. 4431–4435, Jul. 2019, doi: 10.1109/EMBC.2019.8857725.

[3] L. Masia *et al.*, "Soft wearable assistive robotics: exosuits and supernumerary limbs," *Wearable Exoskeleton Systems: Design, control and applications*, pp. 219–254, Mar. 2018, doi: 10.1049/PBCE108E_ch10.

[4] Ikeuchi, Y., Ashihara, J., Hiki, Y., Kudoh, H., Noda, T.: Walking assist device with bodyweight support system. In: IEEE/RSJ International Conference on Intelligent Robots and Systems, pp. 4073–4079, St. Louis, MO, USA (2009)

[5] Y. Kurita, C. Thakur, and S. Das, "Assistive Soft Exoskeletons with Pneumatic Artificial Muscles," in *Haptic Interfaces for Accessibility, Health, and Enhanced Quality of Life*, T. McDaniel and S. Panchanathan, Eds. Cham: Springer International Publishing, 2020, pp. 217–242. doi: 10.1007/978-3-030-34230-2_8.

[6] C. Thalman and P. Artemiadis, "A review of soft wearable robots that provide active assistance: Trends, common actuation methods, fabrication, and applications," *Wearable Technology.*, vol. 1, p. e3, 2020, doi: 10.1017/wtc.2020.4.

[7] "A Recipe for Soft Fluidic Elastomer Robots | Soft Robotics." https://www.liebertpub.com/doi/10.1089/soro.2014.0022 (accessed Dec. 17, 2021).

[8] S. Das and Y. Kurita, "ForceArm: A Wearable Pneumatic Gel Muscle (PGM)-Based Assistive Suit for the Upper Limb," *IEEE Transactions on Medical Robotics and Bionics*, vol. 2, no. 2, pp. 269–281, May 2020, doi: 10.1109/TMRB.2020.2990436.

[9] S. Lessard, P. Pansodtee, A. Robbins, J. M. Trombadore, S. Kurniawan, and M. Teodorescu, "A Soft Exosuit for Flexible Upper-Extremity Rehabilitation," *IEEE Transactions on Neural Systems and Rehabilitation Engineering*, vol. 26, no. 8, pp. 1604–1617, Aug. 2018, doi: 10.1109/TNSRE.2018.2854219.

[10] M. A. Gull, S. Bai, and T. Bak, "A Review on Design of Upper Limb Exoskeletons," *Robotics*, vol. 9, no. 1, Art. no. 1, Mar. 2020, doi: 10.3390/robotics9010016.

[11] E. W. Hawkes, D. L. Christensen and A. M. Okamura, "Design and implementation of a 300% strain soft artificial muscle," 2016 IEEE International Conference on Robotics and Automation (ICRA), 2016, pp. 4022-4029, doi: 10.1109/ICRA.2016.7487592.

[12] B. Tondu, "Modelling of the McKibben artificial muscle: A review," 2012, doi: 10.1177/1045389X11435435.

[13] S. Kurumaya, H. Nabae, G. Endo, and K. Suzumori, "Design of thin McKibben muscle and multifilament structure," *Sensors and Actuators A: Physical*, vol. 261, pp. 66–74, Jul. 2017, doi: 10.1016/j.sna.2017.04.047.

[14] Yukisawa, T., Ishii, Y., Nishikawa, S., Niiyama, R., & Kuniyoshi, Y.. (2017). Modeling of extensible pneumatic actuator with bellows (EPAB) for continuum arm. https://doi.org/10.1109/robio.2017.8324762

[15] Kanno, T., Ohkura, S., Azami, O., Miyazaki, T., Kawase, T., & Kawashima, K.. (2019). Model of a Coil-Reinforced Cylindrical Soft Actuator. Applied Sciences, 9(10), 2109. https://doi.org/10.3390/app9102109

[16] Greer, J. D., Morimoto, T. K., Okamura, A. M., & Hawkes, E. W.. (2017). Series pneumatic artificial muscles (sPAMs) and application to a soft continuum robot. https://doi.org/10.1109/icra.2017.7989648

.